Mammalian Genome 10, 870–878 (1999).

Mammalian Genome
Incorporating *Mouse Genome*

Molecular characterization of radiation- and chemically induced mutations associated with neuromuscular tremors, runting, juvenile lethality, and sperm defects in *jdf2* mice

Mitchell Walkowicz,[1,*] Yonggang Ji,[2] Xiaojia Ren,[1,] Bernhard Horsthemke,[3] Liane B. Russell,[1] Dabney Johnson,[1] Eugene M. Rinchik,[1] Robert D. Nicholls,[2] Lisa Stubbs[1,**]**

[1]Life Sciences Division, Oak Ridge National Laboratory, Oak Ridge, Tennessee 37831-8077, USA
[2]Department of Genetics and Center for Human Genetics, Case Western Reserve University School of Medicine and University Hospitals of Cleveland, Cleveland OH 44106, USA
[3]Institute for Human Genetics, University Clinic Essen, D-4300 Essen 1, Germany

Received: 11 March 1999 / Accepted: 30 April 1999

Abstract. The juvenile development and fertility-2 (*jdf2*) locus, also called runty-jerky-sterile (*rjs*), was originally identified through complementation studies of radiation-induced *p*-locus mutations. Studies with a series of ethylnitrosourea (ENU)-induced *jdf2* alleles later indicated that the pleiotropic effects of these mutations were probably caused by disruption of a single gene. Recent work has demonstrated that the *jdf2* phenotype is associated with deletions and point mutations in *Herc2*, a gene encoding an exceptionally large guanine nucleotide exchange factor protein thought to play a role in vesicular trafficking. Here we describe the molecular characterization of a collection of radiation- and chemically induced *jdf2/Herc2* alleles. Ten of the 13 radiation-induced *jdf2* alleles we studied are deletions that remove specific portions of the *Herc2* coding sequence; DNA rearrangements were also detected in two additional mutations. Our studies also revealed that *Herc2* transcripts are rearranged, not expressed, or are present in significantly altered quantities in animals carrying most of the *jdf2* mutations we analyzed, including six independent ENU-induced alleles. These data provide new molecular clues regarding the wide range of *jdf2* and *p* phenotypes that are expressed by this collection of recently generated and classical *p*-region mutations.

Introduction

The location of a gene(s) required for growth and survival, fertility, and neurological function in proximal mouse Chromosome 7 (Mmu7) was originally deduced through analysis of p^{6H}, a radiation-induced recessive allele at the pink-eyed dilution (*p*) locus (Hunt and Johnson 1971). Although mutations that disrupt the *p* gene alone exert noticeable effects only on the coat and eye color of the animal, a number of radiation-induced *p* mutations produce a complex suite of phenotypes similar to that observed in p^{6H} mice (Lyon et al. 1992; Russell et al. 1995). These mutations have been termed runty-jerky-sterile (*rjs*) alleles by Lyon and colleagues (1992) and p-juvenile lethal (p^{jl}) alleles by Russell and coworkers (1995). The sterility of males homozygous for these alleles (hereafter referred to as p^{jl} alleles) is associated with reduced germ cell numbers and with the production of sperm with multiple, abnormally shaped acrosomes. Binucleate spermatids and "giant" sperm with deformed heads and multiple tails have also been observed (Hunt and Johnson 1971). Although p^{6H}/p^{6H} females are fertile, reproductive features associated with immaturity, such as the presence of polyovular follicles and absence of corpora lutea, have been documented in ovaries of adult p^{6H} mutant mice (Melvold 1974). Pituitary defects observed in association with certain *p*-linked juvenile-lethal alleles have been suggested as contributing factors in reproductive and growth defects observed in these animals (Melvold 1975; Johnson and Hunt 1975).

Studies with the ENU-induced *p*-region mutations have since provided compelling evidence that the neurological abnormalities, genital hypoplasia, sperm head defects, and reduced fitness of p^{6H} and p^{jl}-mutations are due to disruption of a single genetic locus, called juvenile development and fertility 2 (*jdf2;* Rinchik et al. 1995). Recently, one of the radiation-induced *rjs* alleles, p blind-sterile (p^{bs}), was identified as an interstitial deletion in a gene located just proximal of *p* and encoding an exceptionally large, novel protein (Lehman et al. 1998). Single-base splice junction mutations in this same large gene were identified in animals carrying three independent ENU-induced *jdf2* alleles, providing conclusive evidence of the link to the phenotype expressed by *jdf2* mice (Ji et al. 1999). The *Herc2* gene, so-named because it encodes a protein with HECT1 and RCC1 motifs similar to those contained in the guanine nucleotide exchange factor (GEF) protein *Herc1,* encodes a protein of 4836 amino acids and is thought to play a role in vesicular trafficking (Ji et al. 1999). *Herc2* is expressed in most mouse tissues with especially high levels of expression in testis and brain (Lehman et al. 1998; Ji et al. 1999), consistent with the pleiotropic effects that *jdf2* and *rjs* mutations produce in mutant mice.

Most of the radiation-induced, prenatally or neonatally lethal *p*-locus mutations are now known to be deletions (Johnson et al. 1995; Lyon et al. 1992), but molecular defects have not been documented for the majority of p^{jl} alleles. Here we report the analysis of structure and *Herc2* gene expression associated with 13 radiation-induced and 6 ENU-induced *jdf2* alleles. Portions of the *Herc2* transcription unit are deleted or otherwise rearranged in 12 of these radiation-induced mutations, including five of six p^{jl} alleles and several *p*-region mutations that fail to complement p^{jl} alleles but that are associated with homozygous neonatal or prenatal lethality. One radiation-induced mutation, p^{12DTR}, is an interstitial deletion that removes 5015 bp of the 15,247 bp *Herc2* transcription unit; this mutation is also associated with reduced pigmentation, suggesting that this interstitial deletion affects sequences required for the proper expression of *p. Herc2* is transcribed at anomalously low levels in animals carrying five different ENU-induced *jdf2* mutations, including two mutations for

* *Present address:* Laboratory of Pathology, National Cancer Institute, NIH, Bethesda, MD 20892, USA

** *Present address:* Human Genome Center, Lawrence Livermore National Laboratory, 7000 East Avenue, L-452, Livermore, CA 94550, USA.

Correspondence to: L. Stubbs at Livermore

Table 1. Description of p^{jl} and *jdf2* alleles and summary of molecular data.

Allele (reference)	Lethal phenotype[a]	*p* phenotype[b]	Molecular defect	*Herc2* transcript (brain)
$p^{46DfiOD}$ (1,2)[c]	pl	p	Large deletion removing all of *Herc2* and *p*	None detected
$p^{7FR60Lb}$ (1,2)	nl	p	Deletion from *Herc2* nt ~3300 including *p*	None detected
p^{132G} (1,2)	pl	p	Deletion from *Herc2* nt ~3000 including *p*	None detected
p^{116G} (1,2)	nl	p	Deletion from *Herc2* nt ~3300 including *p*	size-altered (6,8 kb), normal quantities
p^{6H} (3)	nd	p	Deletion from *Herc2* nt ~2000 including *p*	None detected
$p^{17FATWb}$ (1)	pl	p^x	Deletion from *Herc2* nt ~2600 ending before 5′-end of *p*	None detected
$p^{12R250M}$ (1)	jm	p^x	Deletion from *Herc2* nt~1600 ending before 5′ end of *p*	None detected
p^{12DTR} (1)	jm	p^x	Interstitial *Herc2* deletion removing 5 kb of coding sequence	Size-altered (~10 kb), reduced quantities
p^{48PB} (1)	pl	p^x	Deletion from *Herc2* nt ~10200 ending before 5′-end of *p*	Truncated (~10 kb), normal quantities
p^{9DTW} (1,2)	jls	p	Deletion from *Herc2* nt ~13300 including 5′-end of *p*	Truncated (~13 kb) Normal quantities
p^{103G} (1)	jm	p^x	Rearrangement detected with *Herc2* nt ~13300–15247	nd
p^{39DSD} (1)	jm	p^m	Rearrangement detected with *Herc2* nt ~7000	nd
p^{16CoS} (1)	jm	p^m	No *Herc2* rearrangement detected	Normal size and quantities
$jdf2^{932SJ}$(4,5)	nd	nd	Point mutation at *Herc2* splice junction	Size nd; increased quantities
$jdf2^{322SJ}$(4,5)	nd	nd	Point mutation at *Herc2* splice junction	Size nd; reduced quantities
$jdf2^{850SJ}$ (4,5)	nd	nd	nd	Size nd; reduced quantities
$jdf2^{1971SJ}$	nd	nd	Point mutation at *Herc2* splice junction	Size nd; reduced quantities
$jdf2^{374SJ}$	nd	nd	nd	Size nd; reduced quantities
$jdf2^{1881SJ}$	nd	nd	nd	Size nd; reduced quantities

[a] Classification of juvenile lethal mild (jlm), severe (jls), neonatal lethal (nl) and prenatal lethal (pl), as described by Russell and colleagues (1995), was determined formally only for the Oak Ridge radiation-induced *p* alleles. Lethal phenotypes for p^{6H} and the six EtNU-induced *jdf2* alleles have not been formally determined, as indicated by "nd" in column 2. Mutations $p^{7FR60Lb}$, p^{132G}, p^{116G}, and $p^{4THO-II}$ are large deletions including the *Gabrb3* gene and are independently associated with neonatal lethality owing to cleft palate (Culiat et al. 1993; Johnson et al. 1995).

[b] Pigmentation phenotypes for the ENU-induced *jdf2* alleles have not been formally determined (nd), since these alleles were induced on *ru2 p* chromosomes (Rinchik et al. 1995). Owing to the predominantly intragenic nature of ENU mutations (Marker et al., 1996), it is highly unlikely that the *p* locus was further mutated in the newly induced *jdf2* chromosomes.

[c] References describing some of these mutations, as indicated in parentheses include 1: Russell et al. 1995; 2: Johnson et al. 1995; 3: Hunt and Johnson 1971; 4: Rinchik et al. 1995; 5: Ji et al. 1999.

which *Herc2* splice junction point mutations have been identified (Ji et al. 1999) and three alleles for which no specific mutations have yet been found. Combined with previously published studies (Lehman et al. 1998; Ji et al. 1999), these results provide new insights into the widely varied expression of juvenile-lethal and pigmentation phenotypes associated with specific *p* and *jdf2* alleles.

Materials and methods

Mutant mice. This study focuses on a series of mutations generated at the *p* locus during specific locus experiments at the Oak Ridge National Laboratory (Russell et al. 1995). Phenotypes associated with each allele analyzed in this study are summarized in Table 1. The Oak Ridge p^{jl} alleles have been classified as mild (*jlm*) or severe (*jls*) juvenile lethal alleles on the basis of average time of death (Russell et al. 1995). The p^{6H} mutation, generated at Harwell, England (Hunt and Johnson 1971), was not included in the Oak Ridge complementation studies. The radiation-induced p^{jl} mutations also express a range of pigmentation defects, including: (1) the fully diluted coat and eye color of *p*-null (or pink-eyed) mutants; (2) the intermediate *p*, or dark-pink-eyed phenotype (p^x), characterized by a moderately diluted coat and dark pink eyes; and (3) a mottled form of *p* (p^m), expressed as light-colored patches of fur against a normally pigmented background (Russell et al. 1995). Also included in this study are several radiation-induced *p* mutations that fail to complement *jdf2* alleles but which delete larger regions including genes with independent effects on prenatal or neonatal survival. These include $p^{46DFiOD}$, a large deletion associated with prenatal lethality owing to deletion of a proximally located early lethal gene, *l7Rl1* (Russell et al. 1995). The p^{116G} and $p^{7FR60Lb}$ deletions that extend distally to include the *Gabrb3* gene and are associated with neonatal lethality due to cleft palate; p^{132G} is also a large deletion associated with homozygous prenatal lethality (Culiat et al. 1993; Russell et al. 1995; Johnson et al. 1995). Two additional alleles, p^{48PB} and $p^{17FATWb}$, fail to complement p^{jl} mutations and are associated with prenatal lethality (Russell et al. 1995) although deletion of proximally or distally located genes have not been reported.

In addition to the radiation-induced mutations, six ENU-induced *jdf2* alleles were also analyzed. These mutations include three *jdf2* mutations described previously ($jdf2^{932SJ}$, $jdf2^{322SJ}$, and $jdf2^{850SJ}$; Rinchik et al. 1995) and three additional mutations described for the first time in this report ($jdf2^{1971SJ}$, $jdf2^{1881SJ}$, and $jdf2^{374SJ}$). These three new *jdf2* alleles were identified and characterized as described previously (Rinchik et al. 1995). *Mus musculus* × *Mus spretus* hybrid animals and compound heterozygotes involving overlapping *p* deletions used for genomic mapping, as well as several p^{jl}/p^{6H} compound heterozygote combinations used for expression analysis, were also generated as described in previous reports (Nicholls et al. 1993; Russell et al. 1995; Johnson et al. 1995).

Molecular probes. The positions of probes used in this study relative to specific portions of the *Herc2* cDNA (Ji et al. 1999) and to a regional P1 contig are summarized in Fig. 1. A 288-bp probe (TADJ5′p) representing the 5′-end of the mouse *p* gene was generated by reverse transcription-polymerase chain reaction (RT-PCR) with primers DJDN10.1 (5′-CACTGCTGGAGAGAGATCAGCGAG-3′; which starts at nt 82 of the mouse *p* cDNA sequence), and DJDN10.2 (5′-CGTTTTCTCTGAGGAG-GCAACTGCAGA-3′; reverse complement from nt 469 of the *p* gene sequence published by Gardner et al. 1992). First-strand cDNA was generated from 2 μg mouse total brain RNA and was primed with random hexamers using Superscript reverse transcriptase (Gibco-BRL; Gaithersburg, Md.) according to manufacturer's instructions. The mupc78.5 cDNA is a 2.0-kb clone isolated from an E8.5-day post coitum mouse embryo library (Brigid Hogan and colleagues, unpublished) with the human cDNA pc7.541 probe (Buiting et al. 1992). RNase protection experiments were carried out with probe E550, a 703-nt *Eco*RI–*Pst*I fragment corresponding to *Herc2* nucleotides 4085–4788. Northern blots were hybridized with 5504K, a 4.7-kb cDNA clone isolated from a size-selected, oligo dT-primed mouse 14-day postnatal cerebellum cDNA library (Doyle et al. 1997) corresponding to *Herc2* nucleotides 1758–6472. Probes YJ1.7 and YJ1.1 are human probes derived from highly conserved 5′-portions of human HERC2 cDNA sequence (Ji et al. 1999). YJ1.7 contains HERC2 nt 1638–2612, while YJ1.1 contains nt 2613–3704. RN5561.9 and RN5562.3 are *Eco*RI subclones generated from a 4.1-kb mouse cDNA clone isolated from the cerebellum library with a human HERC2 probe (RN556; Ji et al. 1999). RN5561.9 represents nt 6204–8104, and RN5562.3 corresponds to nt 8105–10,200 of the *Herc2* cDNA sequence. The YJ7KCD probe was a 7-kb RACE product representing the 3′-end of the mouse *Herc2* gene (nt 8302–15,247); 1.5PA+ is a 1.595-kb subclone generated from YJ7KCD and corresponds to the 3′-terminal end of the *Herc2* transcript (nt 13,644–15,247 and 17 polyA residues; Ji et al. 1999).

Genomic clone isolation and characterization. Bacteriophage P1 clones used in this study were isolated by hybridization of high-density gridded arrays of a library constructed from C57BL/6 mouse DNA (F.

Francis, unpublished) and distributed by the Reference Library Database (RLDB; Max Planck Institute for Molecular Genetics, Berlin-Dahlem, Germany). P1 endclones were generated by a modified version of the ligation-mediated PCR technique originally described by Mueller and Wold (1989). Briefly, DNA was prepared from P1-containing colonies by standard alkaline lysis methods. Approximately 0.2 μg of each DNA preparation was digested with *Eco*RV, *Rsa*I, and either *Taq*I or *Pst*I for left or right vector ends, respectively. After digestion, the DNA was phenol extracted, precipitated, and washed with 70% ethanol, and the pellet resuspended in 10 μl TE. Two μl of each digest was ligated to 5 pmol of annealed linker (oligonucleotides L and LP; Mueller and Wold 1989) in a 10-μl reaction at 14°C overnight. Two μl of the ligated material was used as template in a 100-μl PCR reaction, with 100 ng each of either LP and standard T7 oligonucleotides, or LP and SP6, as primers (to represent sequences located to the "left" and "right" of the P1 cloning site, respectively). Samples were amplified in 35 cycles at an annealing temperature of 65°C. Two μl of the primary PCR reaction was reamplified with the same primers and conditions as above. The resulting endclone products were purified from low-melting-point agarose. The 5′-*p*-containing cosmid was isolated by hybridization of the TADJ5′p probe to a cosmid library generated by *Mbo*I partial digestion of mouse genomic DNA (from a mouse homozygous for the $Mgf^{Sl\text{-}74G}$ mutation) and cloned into the pCos2 vector (L. Stubbs, unpublished).

DNA sequencing and hybridizations. Restriction enzyme-digested genomic and P1 clone DNA samples were electrophoresed through 0.8% agarose gels and blotted to nylon filters. Filters were hybridized with radiolabeled probes as previously described (Stubbs et al. 1990); repetitive probes were preassociated with both sheared mouse genomic DNA and/or Cot-1 DNA (Gibco BRL) as described in the same reference. cDNA clones mupc78.5 and jsub5.1 were subcloned into the pBSKII+ vector (Stratagene, La Jolla, Calif.) and partially sequenced with a combination of manual (Sequenase 2.0 USB) and automated fluorescence-base methods (Prism Dye Terminator Cycle Sequencing Ready Reaction kit; PE Applied Biosystems, Foster City, Calif.). Fluorescently labeled reactions were analyzed on a PE-ABI 373 automated sequencer, according to manufacture's instructions. Sequences were analyzed with GCG software, version 7 (Genetics Computer Group Inc., Madison, Wis.).

RNA isolation, Northern blotting, and RNase protection. Total RNA was isolated and oligo-dT selected with commercially available kits (5 Prime 3 Prime, Inc., Boulder, CO). PolyA$^+$ RNA (~2.5 μg per lane) was electrophoresed though 0.8% agarose gels containing 19% formaldehyde, soaked 30 min in 50 mM NaOH, neutralized briefly in 0.1 M Tris-HCl, and blotted to Duralon nylon membranes (Stratagene) in 20× SSC after electrophoresis. Blots were rinsed in 2× SSC and baked 2 h under vacuum, and UV crosslinked at 250 μjoules/mm^2 in a Stratalinker (Stratagene) before hybridization. RNase A protection assays were performed with the RPAII kit (Ambion, Inc., Austin, Tex.) essentially as per manufacturer's instructions. Briefly, 10 μg total RNA was hybridized overnight with ~5.0×10^4 cpm of ^{32}P-UTP-labeled E550 subclone and β-actin control (the latter provided by the manufacturer). Hybrids were digested with RNase A, and digests were precipitated and resolved on a 5% denaturing polyacrylamide gel. Gels were exposed by the Phosphorimager II system (FuJItsu, Inc., Tokyo, Japan), and dosimetric analysis was performed using MacBas software.

Isolation of sequences flanking the p^{12DTR} deletion breakpoint. RT-PCR was performed to identify the *Herc2* cDNA deletion in p^{12DTR} mutant mice. Total RNA was isolated from brain of p^{12DTR}/p^{6H} mice and reverse transcribed into cDNA with MMLV-reverse transcriptase (GIBCO-BRL, Gaithersburg, Md.). RT-PCR with oligonucleotide primers RN569 (5′-CCAGGCATACTTTCGGCAGGATTA-3′, from nt 8302 of *Herc2*) and RN668 (Ji et al. 1999; 5′-ATTGTCTCCAGTTCGTATCC-3′, ends in nt 14095 of *Herc2*) amplified a p^{12DTR} cDNA fragment of 0.78 kb. Long-range genomic PCR was performed to identify the ends of the deleted genomic segment in p^{12DTR}. DNA from BAC clone B1 was used as control to amplify the wild-type genomic sequences. The 5′ intron was amplified with RN569 and RN814 (5′-GCTTTTCACCATTCGGGACCAG-3′, ends in nt 8438). The 3′ intron was amplified with RN694 (5′-AGCTTTCAGGAAGGTAGTACAAGC-3′, starts from nt 13271) and RN692 (5′-AAAGACAGACTTGGTGCCATCAGG-3′, ends in nt 13409). To amplify the 12DTR genomic sequence, genomic DNA was isolated from brain of $p^{12DTR}/p^{7FR60Lb}$ mice. Genomic sequence from the p^{12DTR} allele was amplified with primers RN569 and RN692, described above. All of the genomic fragments were amplified by two step PCR of 30 cycles with 5 min annealing and extension, with TaKaRa LA PCR Kit (TaKaRa Biomedicals, Shiga, Japan).

Results

Generation of a P1 clone contig in the Herc2–p interval. Recent molecular studies have located the 3′-terminus of *Herc2* gene very near to and proximal of the 5′-end of *p* (Lehman et al. 1998; Ji et al. 1999). Since the radiation-induced *jdf2* alleles were originally selected for study because of their effects on pigmentation (Russell et al. 1995), each also affects sequences required for normal *p* gene expression. To provide tools that would permit each mutation to be mapped with respect to both genes and intervening regulatory sequences, we constructed a clone-based physical map of the *Herc2–p* genomic interval. Probes pTADJ5′*p* (representing the 5′-end of *p*) and mupc78.5 (a 2-kb partial mouse cDNA clone corresponding to the central region of the *Herc2* gene) were used to isolate bacteriophage P1 clones from a mouse genomic library. Since initial analyses indicated that mupc78.5-containing clone, ICRFP703N21306 (abbreviated N2), and 5′-*p* positive P1 clone, ICRFP703N15109 (N1), did not overlap, we generated end-probes from the P1 clones and used those probes to identify an additional P1 clone (ICRFP703B11152, abbreviated clone B1). Clones B1, N1, and N2 were confirmed by endclone hybridization to form a contiguous overlapping set. Each clone contains ~85 kb of mouse genomic DNA (as estimated by summing restriction fragment lengths in several different digests for each clone). Comparison of restriction enzyme digest patterns and probe hybridization data (see below) indicated that the three clones span an estimated total distance of 160–180 kb (Fig. 1B).

As full-length human and mouse HERC1/*Herc1* cDNA clones were derived (Ji et al. 1999), we used probes representing specific fragments of the transcribed sequence (Fig. 1A) to map portions of the gene within the P1 contig (Figs. 1, 2). *Herc2* sequences are distributed throughout the length of the contig, although a probe representing the extreme 5′-end of *Herc2* (sequences corresponding to *Herc2* nt 1–451) is not present in the three overlapping clones. As demonstrated by Lehman and colleagues (1998), our data indicate that the 3′-end of *Herc2* and the 5′-end of *p* are located close together in mouse, as has also been observed for the related genes in human (Ji et al. 1999). Although the precise distance between *Herc2* and the 5′-end of *p* cannot be determined from these data, previous reports have estimated the two genes to lie ~10 kb apart (Lehman et al. 1998), a finding that is fully consistent with mapping data presented here. Since the majority of the p^{jl} mutations involved sequences located in the interval between *Herc2* and *p* (see below), we did not endeavor to extend the clone contig to include the 5′-end of *Herc2* as part of the present study.

Rearrangements detected by Herc2 cDNA fragments and P1 endclones in animals carrying radiation-induced jdf2 alleles. To identify and map DNA rearrangements associated with specific p^{jl} mutations, P1 endclones and *Herc2* cDNA sequences were hybridized to DNA derived from animals carrying various radiation-induced *p* alleles. The TADJ5′*p* probe also was analyzed. Results of selected hybridizations are shown in Fig. 2, and data derived from a more complete series of Southern blot analyses are summarized in Table 2. The map resulting from these combined analyses is summarized in Fig. 1B. End clones located internally within the P1 contig (N1-T7, N2-T7, B1-SP6, and B1-T7) are deleted in several p^{jl} mutations including p^{48PB}, p^{12DTR}, $p^{12R250M}$, and $p^{17FATWb}$, in which DNA rearrangements had not been detected previously. Both breakpoints of several deletions including p^{9DTW},

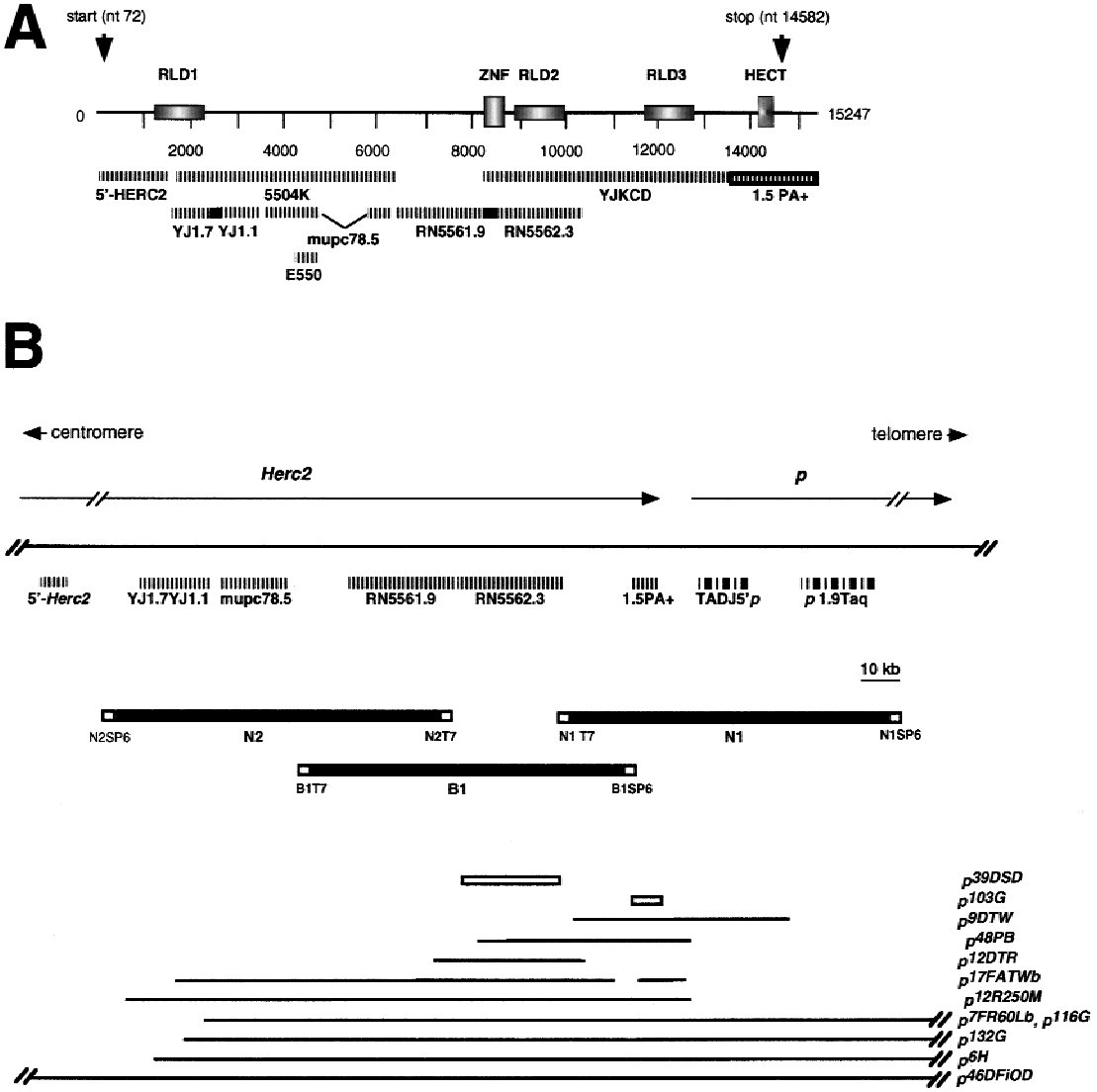

Fig. 1. Location of specific *Herc2* cDNA probes and summary map of the *jdf2* contig region. **(A)** Location of human and mouse molecular probes relative to the 15247-bp mouse *Herc2* transcript. Map at top represents the *Herc2* transcript, with the 5′-end at far left. Numbers under the map indicate nucleotide positions in the cDNA sequence (Ji et al. 1999). The contents of specific cDNA fragments used in these studies are indicated by hatched lines below the map, with probe names indicated below. Subclones used in specific experiments are indicated by a box drawn over the pertinent portion of that larger fragment. Probes YJ1.7 and YJ1.1 are restriction fragments derived from a single larger clone; the dark bar between these two probes indicates the approximate position of the restriction site. cDNA clone mupc78.5 contained two non-contiguous segments of the complete *Herc2* coding sequence, as indicated by the bracket joining the two aligned fragments; this possibly reflects that the gene is alternatively spliced. Symbols overlaid on the transcript map indicate the approximate positions of sequences representing conserved protein motifs in the HERC2 protein (Ji et al. 1999). These include: RLD1, RLD2, RLD3, representing RCC1-like repeats; ZNF, representing a zinc finger motif; and an N-terminal HECT, or E3 ubiqitin ligase domain. Positions of the translational start and stop codons are also indicated. **(B)** Summary physical and deletion map of the *jdf2* region. Top line represents the *Herc2–p* interval of mouse Chr 7, with centromeric/telomeric orientation, extents, and transcriptional direction (arrows) of the *Herc2* and *p* genes indicated. Solid bars below indicate the positions of overlapping P1 clones, N2, B1, and N1; P1 end-probes are represented by open boxes at the end of each clone. The precise locations of specific exons detected by specific *Herc2* and *p* cDNA probes are not known; approximate extents of genomic sequences detected by each probe, defined by P1 clone and deletion overlap, are indicated by hatched bars above the P1 contig. Positions of rearrangements detected by cDNA and P1 end probes in specific radiation-induced *p* mutations are indicated below the map, with the name of each mutation listed at right. Lines indicate the positions of deletions, while open rectangles indicate intervals within which size-altered fragments were detected without obvious signs of deletion.

p^{12DTR}, p^{48PB}, and $p^{12R250M}$ are contained entirely within the boundaries of the cloned region (Table 2; Figure 1B).

Hybridization analysis of *Herc2* coding sequences also revealed the positions of breakpoints of several *jdf2* alleles and provided clues to their effects on *Herc2* and *p* function. A probe representing the 3′-most 1.5 kb of *Herc2* transcript (1.5PA+) is deleted in the p^{9DTW} allele; other *Herc2* exon-containing probes are unaffected in this mutant (Figs. 1B, 2B; Table 2). The proximal end of the p^{9DTW} deletion is defined by rearranged restriction fragments detected with the N1T7 endclone probe (Fig. 2B; Table 2). p^{9DTW} is associated with a severe form of the juvenile-lethal phenotype and, consistent with its pink-eyed phenotype, also deletes the 5′-end of *p* (Table 2; Johnson et al. 1995). Hybridization studies also showed that the p^{48PB} deletion extends from *Herc2* nt ~10,200 to the end of the transcription unit. Although p^{48PB}/p compound heterozygotes express a p^{x} phenotype (Table 2), this mutation does not appear to affect the structure of *p* coding sequences (Table 2; Fig. 1B). Interestingly, despite the relatively

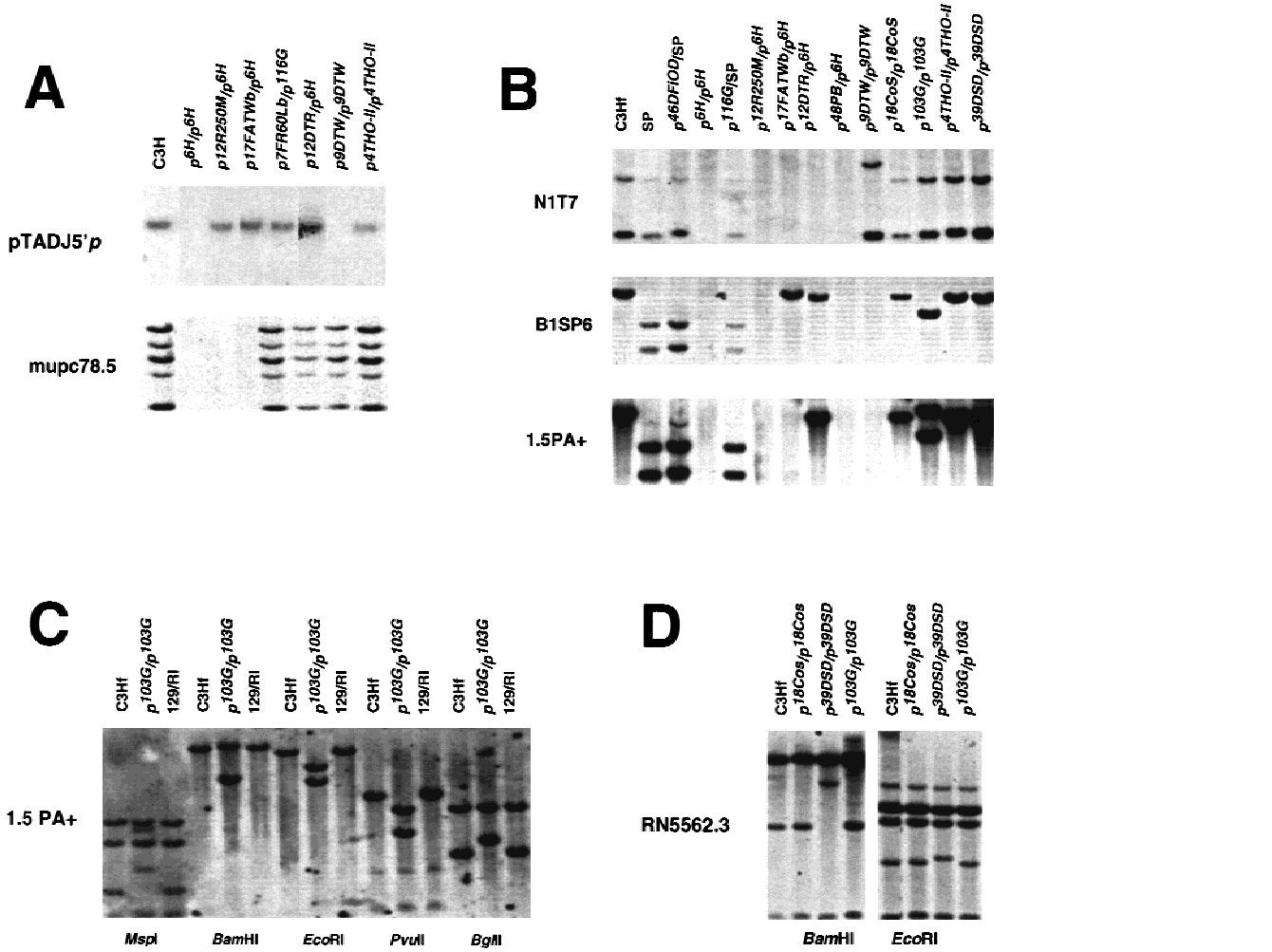

Fig. 2. Hybridization of *jdf2*-region gene markers and P1 end probes to DNA isolated from animals carrying radiation-induced *p* alleles. Southern blots carrying restriction enzyme-digested DNA samples taken from mice of various genotypes were hybridized with *p, Herc2,* and P1-endclone probes. Symbols representing the genotype, species, or strain of animals from which each DNA sample was isolated (*p* and *jdf2* alleles, described in Table 1; background mouse strains St2A, C3Hf, 129/R1; or SP (= *Mus spretus*) are represented above each set of aligned panels. Names of probes used for hybridizations are shown at left of each panel. **(A)** Presence or absence of sequences corresponding to the 5′-end of *p* (pTADJ5′*p*) and internal portions of *Herc2* (represented by subtracted cDNA fragment, jsub5.1) in *Eco*RI-digested DNA derived from animals carrying a selection of radiation-induced *p* alleles. **(B)** Hybridization of P1 end probes N1T7 and B1SP6, and 3′-*Herc2* probe 1.5PA+, to *Pst*I-digested DNA samples, from control animals as well as homozygous *jdf2* mutants or compound heterozygotes, and hybrid animals generated by crossing *M. musculus* females carrying *p* alleles with *M. spretus* males (e.g. p^{116G}/SP). **(C)** Size-altered fragments detected by the 1.5PA+ probe in p^{103G}/p^{103G} mutant animals. Fragments of altered size were detected in digests of p^{103G}/p^{103G} DNA samples with all restriction enzymes tested. **(D)** Hybridization of *Herc2* internal cDNA fragment, RN5562.3, to *Bam*HI and *Eco*RI-digested DNA from mice of various genotypes as indicated in the figure. Rearranged restriction fragments detected in *Bam*HI and *Eco*RI digests of DNA isolated from p^{39DSD} homozygotes are shown.

small deletion detected in these mutants, p^{48PB} is classified as a prenatal lethal allele (Russell et al. 1995; Table 2).

The $p^{17FATWb}$ mutation is also classified as a prenatal lethal mutation, although it deletes a slightly smaller portion of the *Herc2* transcription unit than does the mild juvenile lethal allele, $p^{12R250M}$ (Table 1; Fig. 1B). However, hybridization data suggested that $p^{17FATWb}$ might represent a complex rearrangement as opposed to a single contiguous deletion. Sequences detected by the B1SP6 endclone probe are present and are of normal size in $p^{17FATWb}$ DNA samples, whereas sequences located both proximal (e.g., RN5562.3) and distal (e.g., 1.5PA+) of the endclone sequence are deleted in $p^{17FATWb}$ mutant DNA (Table 1; Fig. 2B). The B1SP6 end clone fragment contains *Herc2* coding sequences that are located 5′- of the 1.5PA+ probe, as demonstrated by DNA sequencing data (R. Uphoff, personal communication), confirming the 5′-3′ order of these two probes. These data raise the possibility that $p^{17FATWb}$ might represent a complex "skipper" mutation or correspond to a complex inversion/deletion event.

Molecular characterization of an intragenic Herc2 deletion in p^{12DTR} mutant mice. Mice homozygous for the p^{12DTR} mutation express a mild juvenile-lethal phenotype and an intermediate level of pigmentation (Russell et al. 1995). Hybridization data indicated that p^{12DTR} is an interstitial deletion, removing nt ~8000–13,300 of the *Herc2* coding sequences while leaving the 5′-half and 3′-end of the gene intact. Probes RN5562.3 (representing HERC2 nt 8105–10,200) and most sequences detected by the 7-kb 3′-terminal RACE product probe, YJ7KCD, are deleted in p^{12DTR} mutant DNA. Probe RN5561.9 (containing HERC2 nt 6204–8104) detects rearranged restriction fragments in p^{12DTR} DNA, whereas genomic sequences detected by 5′-*Herc2* probes YJ1.1 and YJ1.7 and 3′-terminal probe 1.5PA+ are not altered in these mutants (Figs. 1B, 2B).

To define the boundaries of the p^{12DTR} deletion, we performed RT-PCR, using *Herc2* primer pairs chosen to surround the predicted deleted region with cDNA templates prepared from p^{12DTR} mutant mice. The product produced from p^{12DTR} cDNA samples

Table 2. Summary of hybridizations of P1 end-probes and *Herc2* cDNA fragments to DNA isolated from animals carrying radiation-induced p^{jl} mutant alleles.

Probe Allele	N2 SP6	YJ1.7	YJ1.1	mupc- 78.5	B1T7	RN556 1.9	N2T7	RN556 2.3	N1T7	B1 SP6	1.5- PA+	pTAD- J5′p	N1 SP6
$p^{46DFiOD}$	D	D	D	D	nd	D	D	D	D	nd	D	D	D
$p^{7FR60Lb}$	+	+	P	D	D	D	D	D	D	D	D	D	D
P^{132G}	+	+	P	D	D	D	D	D	D	D	D	D	D
p^{116G}	nd	+	P	D	D	D	D	D	D	D	D	D	D
p^{6H}	+	P	D	D	D	D	D	D	D	D	D	D	D
$p^{12R250M}$	+	D	D	D	D	D	D	D	D	D	D	+	+
$p^{17FATWb}$	+	+	D	D	D	D	D	D	D	+	D	+	+
p^{12DTR}	+	+	+	+	+	P	D	D	D	+	+	+	+
p^{48PB}	+	+	+	+	+	+	+	D	D	D	D	+	+
p^{9DTW}	+	+	+	+	+	+	+	+	R	D	D	D	+
p^{103G}	+	+	+	+	+	+	+	+	+	+	R	+	+
p^{39DSD}	+	+	+	+	+	+	+	R	+	+	+	+	+
p^{18CoS}	+	+	+	+	+	+	+	+	+	+	+	+	+

D, deleted; P, partially deleted (one or more restriction fragments absent); R, rearranged (restriction fragment(s) of abnormal length detected); +, normal restriction fragments detected; nd, not determined. N2SP6, N2T7, B1SP6, B1T7, N1SP6, and N1T7 are end-probes derived from P1 clones N2, B1, and N1, respectively; other probes are Herc2/HERC2 cDNA fragments. See Fig. 2 for summary and additional details.

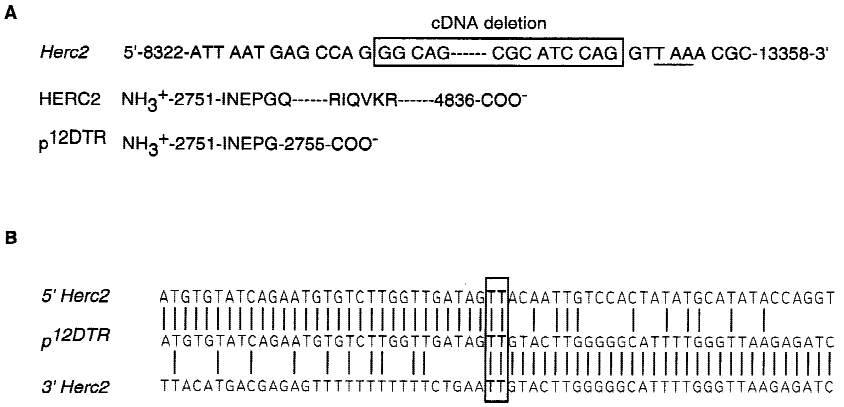

Fig. 3. Molecular characterization of the p^{12DTR} mutant. **(A)** The p^{12DTR} mutation deletes 5015 bp of the *Herc2* cDNA sequence (GenBank accession: AF071173). The *Herc2* wild-type nucleotide sequence is arranged to show the codon structure. Boxed sequences are deleted in the p^{12DTR} allele, leading to a frameshift and premature stop codon (underline). The translated wild-type HERC2 amino acid sequences as well as the truncated sequence in p^{12DTR} are also shown. **(B)** The genomic sequences flanking the 5′ and 3′ p^{12DTR} deletion breakpoints are unique. Top: intronic sequence from the 5′ intron around the deletion breakpoint; bottom, sequence from the 3′ intron; middle: recombinant intronic sequence in the p^{12DTR} mutant allele. The boxed region indicates the position of the crossover.

was significantly shorter (780 bp) than the predicted length of the *Herc2* cDNA segment between these primer sequences (5795 bp). Alignment of the p^{12DTR} RT-PCR product sequence with the normal transcript revealed a 5015 deletion of *Herc2* coding sequences in the p^{12DTR} cDNA, extending from *Herc2* nucleotide 8335 to 13349 (Fig. 3A). This deletion is predicted to cause a frameshift in the *Herc2* coding sequence and premature termination of protein translation, since the first codon after the deleted sequence in p^{12DTR} is a TAA stop codon. The mutant protein produced from this deleted mRNA thus can be predicted to lack the second and third RLD domains as well as the HECT domain present in the intact version of HERC2 (Fig. 1A; Ji et al. 1999).

We also used PCR primers designed from *Herc2* cDNA around the deletion to amplify and characterize the breakpoint region in normal and p^{12DTR} genomic DNA. These analyses showed that both breakpoints of the p^{12DTR} deletion are located in *Herc2* introns. In normal control mice, the intron located just 5′ of the deleted region (between cDNA nt 8334 and 8335) is ~3.5 kb in length, whereas the intron located 3′- of the deleted exons (between nt 13349 and 13350) spans ~3.7 kb (data not shown). In p^{12DTR} mutant mice, portions of these introns are joined to create a contiguous intronic sequence of 4.4 kb. We PCR generated, cloned, and sequenced part of each normal intron in order to identify the p^{12DTR} breakpoint site. The sequences surrounding the deletion ends are unique, and there is no significant sequence similarity between the 5′ and 3′ flanking sequences except for two shared nucleotides at the breakpoints (Fig. 3B).

Rearrangements detected in other p^{jl} alleles. Size-altered fragments were detected by the 3′-*Herc2* probe, 1.5PA+, in all p^{103G}/p^{103G} restriction enzyme digests examined (Fig. 2C). Although the precise nature of the rearrangement detected in these mutants was not determined, the increased number of fragments and/or patterns of size-altered restriction fragments detected with the 1.5PA+ probe suggests the presence of a small insertion or duplication near the 3′-end of *Herc2*. Nevertheless, no altered *Herc2* cDNA sequences were identified (data not shown). Size-altered restriction fragments were also detected in p^{39DSD}/p^{39DSD} DNA samples with probe RN5562.3 (Fig. 2D). *Herc2* cDNA sequences and regional P1 end-probes failed to detect DNA rearrangements in one of the alleles tested, p^{18CoS}, which, like p^{39DSD}, is also associated with mottled pigmentation and a mild *jdf2* phenotype (Russell et al. 1995; Table 2). Further analysis of sequences within the *Herc2*–*jdf2* interval will be required to establish the molecular basis of this mutation.

Expression of Herc2 in mouse embryos and in p^{jl} mutants. *Herc2* produces a >15-kb transcript in most mouse tissues with relatively high levels of expression in brain and testis (Nicholls et al. 1993; Lehman et al. 1998; Ji et al. 1999) and ovary (M. Walkowicz, unpublished). A similar pattern of nearly ubiquitous expression has been documented for the human HERC2 gene (Ji et al. 1999). RNase protection experiments demonstrated that *Herc2* is also expressed at high levels during mouse prenatal development, with significant levels of transcription seen as early as 12.5 dpc (Fig. 4A). Since the *Herc2* cDNA clone, mupc78.5, was isolated as the longest of numerous positive clones present in a 8.5-dpc embryo library, it is likely that *Herc2* transcripts are also expressed at significant levels during earlier stages of mouse development.

In order to provide additional information regarding *Herc2* function and dysfunction in p^{jl} and *jdf2* mutants, we hybridized the

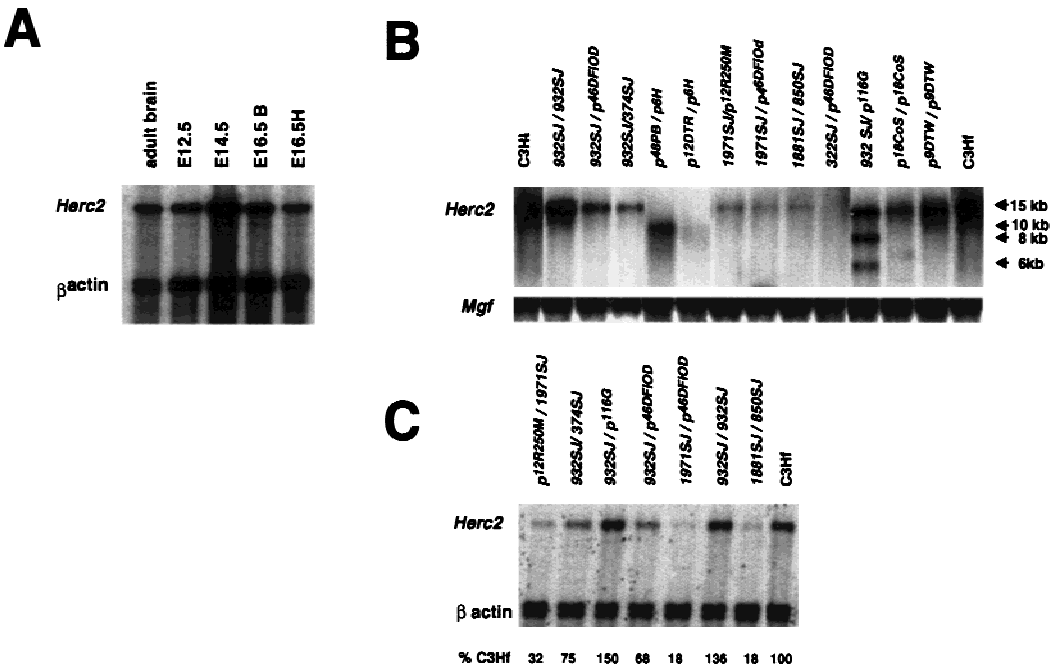

Fig. 4. *Herc2* gene expression in normal and mutant mouse tissues. **(A)** RNase protection of *Herc2* transcript in embryos and adult brain. RNA prepared from adult brain, whole 12.5 d.p.c. and 14.5 d.p.c. embryos, and 16.5 d.p.c. embryos dissected into two parts (bodies, [B], and isolated whole heads, [H]) was protected with the E550 cDNA fragment, as described in the text. β-actin protection probes were also added to provide internal quantitation controls for each sample. **(B)** Expression of *Herc2* mRNA in *jdf2* mutant brain. *Herc2* cDNA probe was hybridized to a Northern blot carrying PolyA$^+$ RNA isolated from brains of animals carrying a selection of *jdf2* mutant alleles. The genotype of animals from which each tissue sample was taken is shown above the pertinent gel lane. For simplicity, *jdf2* alleles included in the genotypes are designated above each lane only by their specific allele identifiers (e.g. *932SJ* vs *jdf2*^{932SJ}). The approximate sizes of transcripts detected in each mutant are indicated by arrows at right. A probe for the *Mgf* gene, which also detects a large transcript (~6 kb) in brain, was hybridized to the same Northern blot to provide a control for RNA quantity and integrity. **(C)** Detection and quantitation of *Herc2* transcript in brains of animals carrying ENU-induced *jdf2* mutations. RNase protection was performed with the E550 probe with RNA isolated from brain of mice carrying ENU-induced *Herc2* mutations as homozygotes or as compound heterozygotes with deletions or with ENU-induced mutations. Autoradiographic signals produced by each mutant transcript were normalized relative to internal β-actin controls, and normalized *Herc2* mRNA quantities detected in mutant brains were measured as a percentage of *Herc2* transcript detected in brains of normal C3Hf mice.

5504K mouse cDNA clone to a Northern blot containing RNA isolated from brains of mice carrying a selection of p^{jl} alleles (Fig. 4B). In addition to the radiation-induced alleles, we also analyzed a total of six ENU-induced *jdf2* mutations: *jdf2*^{322SJ}, *jdf2*^{932SJ}, *jdf2*^{850SJ}, *jdf2*^{1881SJ}, *jdf2*^{1971SJ}, and *jdf2*^{374SJ}. Expression of *Herc2* was also investigated in a larger collection of mutant animals with RNase protection with the E550 probe (Fig. 4C). For reasons related to mutant availability, many *jdf2* alleles were analyzed in compound heterozygotes, and this fact complicated interpretation of expression data to some degree. However, several clear conclusions regarding mutant gene expression can be deduced. Since most or all of the *Herc2* transcription unit is deleted by the p^{6H}, $p^{46DFiOD}$, $p^{12R250M}$, and $p^{7FR60Lb}$ mutations, chromosomes carrying these alleles did not yield *Herc2* mRNA species that could be detected by this RNase protection assay. Truncated forms of the transcript might indeed be produced by certain of these deleted alleles; for example, a short transcript containing 1993 nucleotides of the *Herc2* transcript was isolated from p^{6H}/p^{6H} brain RNA samples with RACE (Lehman et al. 1998). However, such short transcripts would not be detected with the relatively 3′-cDNA probes that we used in this study. Transcripts detected by the 5504K and E550 probes in compound heterozygotes involving these larger deletions therefore represent mRNA contributed by the second allele involved in the cross. Animals inheriting a deletion together with a normal chromosome (e.g. p^{6H}/+) can be expected to produce 50% of the levels of *Herc2* transcript isolated from normal mice (+/+). Compound heterozygotes that carry one deleted chromosome and a *jdf2* allele that affects expression or stability of the *Herc2* transcript should, therefore, yield significantly less than 50% of the normal levels of *Herc2* mRNA.

From integration of data derived from Northern blot and RNase protection experiments, it can be deduced that most *jdf2* mutant alleles examined are associated with defects in *Herc2* gene expression, either by affecting steady-state levels of the transcript or by altering the size of mRNA species produced (Fig. 4B, 4C; summarized in Table 1). Steady-state levels of *Herc2* mRNA were reproducible in repeated experiments with animals carrying any one allele and were verified through analysis of animals carrying different allelic combinations. For example, while the p^{48PB} deletion produces normal quantities of *Herc2* transcript (*Herc2* mRNA is present in p^{48PB}/p^{6H} brains at 50% wild type levels; data not shown), the mRNA produced by the p^{48PB} allele is significantly shorter in length than the mRNA expressed by normal animals (Fig. 4B). A smaller mRNA is also produced in p^{12DTR} mutants, although transcription levels and/or mRNA stability also appear to be affected by this interstitial deletion. Since *Herc2* transcripts are present at relatively high levels in these mutants, it is possible that truncated forms of the *Herc2* protein are also produced in tissues of p^{48PB} and p^{12DTR} mice.

Similarly, since *jdf2*^{932SJ} homozygotes produce a transcript of normal length, the ~6-kb and ~8-kb *Herc2* mRNA species produced by *jdf2*$^{932SJ}/p^{116G}$ compound heterozygotes must be products of the radiation-induced p^{116G} allele (Fig. 4B). Since p^{116G} is a deletion extending from the 5′-end of *Herc2* (beginning at nt ~2500 of the transcript) distally to include all of *p* and *Gabrb3* (Johnson et al. 1995), these smaller mRNA species may represent

the fusion of 5′-*Herc2* sequences with 3′-portions of a gene located distal to *Gabrb3*.

Six ENU-induced jdf2 alleles yield altered steady-state levels of Herc2 transcript. In addition to mutations producing transcripts of altered length, several *jdf2* alleles appear to affect either levels of transcription or stability of the *Herc2* mRNA (Fig. 4C; Table 1). Interestingly, several alleles in this class are ENU-induced mutations. For example, $jdf2^{1971SJ}/p^{46DFiOD}$ and $jdf2^{1971SJ}/p^{12R250M}$ compound heterozygotes produced 18% and 32% of the normal quantity of *Herc2* mRNA, respectively (Fig. 4C). Because $p^{46DFiOD}$ and $p^{12R250M}$ delete most or all of *Herc2* coding sequences, the $jdf2^{1971SJ}$ chromosome can be deduced to yield 36–64% of the normal levels of *Herc2* mRNA (~50% as averaged over several independent RNase protection experiments). Similarly, $jdf2^{1881SJ}/jdf2^{850SJ}$ compound heterozygotes produced only 18% of normal levels of *Herc2* transcript (Fig. 4C). Although the precise contribution of each mutation cannot be deduced from these data, this level of transcript requires that both alleles yielded significantly reduced quantities of *Herc2* mRNA. One ENU-induced mutation, $jdf2^{932SJ}$, consistently produced higher-than-normal levels of *Herc2* transcript. In one experiment, homozygous $jdf2^{932SJ}/jdf2^{932SJ}$ mice produced 138% wild-type levels of *Herc2* mRNA; similarly, high levels of transcript were observed in independent assays of animals carrying the $jdf2^{932SJ}$ allele. For example, a hemizygous mutant, $jdf2^{932SJ}/p^{46DFiOD}$, yielded 68% normal *Herc2* mRNA levels (Fig. 4C and data not shown). Tissues from the compound heterozygote, $jdf2^{932SJ}/jdf2^{374SJ}$, yielded 75% normal transcript levels, suggesting that the $jdf2^{374SJ}$ allele contributed little or no *Herc2* mRNA in compound mutant tissues (Fig. 4C).

Discussion

Data presented in this manuscript provide the first molecular characterization of a group of radiation-induced alleles associated with the long-studied p^x, p^m, and p^{jl} (*jdf2*) mutant phenotypes, and define more precisely the breakpoints of molecular rearrangements associated with several previously characterized *p*-region mutations. Six of seven radiation-induced alleles associated with the *jdf2* phenotype when homozygous, and five prenatal or neonatal lethal deletions that fail to complement *jdf2* mutations, are rearrangements affecting the structure and/or expression of the *Herc2* gene. One *jdf2* allele, p^{12DTR}, was shown to represent an interstitial deletion within the *Herc2* transcription unit.

Animals carrying several different *jdf2* alleles express abnormal levels of the *Herc2* transcript; five of the six ENU mutations we studied are members of this mutant class. While brains of five ENU mutants consistently yielded lower-than-normal quantities of *Herc2* mRNA, tissues isolated from mice carrying one ENU-induced allele, $jdf2^{932SJ}$, were found to express *Herc2* at abnormally high levels. The $jdf2^{322SJ}$, $jdf2^{1971SJ}$, and $jdf2^{932SJ}$ alleles have been shown to represent splice-junction point mutations that cause adjacent exons to be omitted and/or mis-spliced in the mutant transcripts (Ji et al. 1999). The $jdf2^{322SJ}$ and $jdf2^{1971SJ}$ mutations are associated with translational frameshifts predicted to cause premature termination of mutant *Herc2* proteins, and reduced levels of *Herc2* mRNA levels observed in both mutants are probably owing to decreased transcript stability associated with these premature stops (Maquat 1996). By contrast, exon-skipping in the $jdf2^{932SJ}$ allele produces an in-frame deletion, and the mutant mRNA is predicted to produce a protein that is nearly full-length but missing a segment of only 53 amino acids (Ji et al. 1999). The higher levels of *Herc2* transcript observed in $jdf2^{932SJ}$ mutants relative to normal mice cannot be explained by present data. However, the fact that $jdf2^{932SJ}/jdf2^{932SJ}$ animals exhibit a clear *jdf2* phenotype despite expression of a stable, nearly full-length transcript suggests that the deleted exon(s) must encode a peptide segment required for full function of the HERC2 protein. The molecular basis of the lower levels of transcript detected in $jdf2^{1881SJ}$, $jdf2^{850SJ}$, and $jdf2^{374SJ}$ has not yet been determined and is the subject of continuing study.

Data presented here provide satisfying molecular explanations for the effects of many *jdf2* alleles, but several interesting puzzles remain. For example, $p^{12R250M}$ homozygotes express a mild form of the *jdf2* phenotype despite the fact these animals are deleted for nearly all of *Herc2* coding sequences. By contrast, p^{9DTW} and p^{48PB}, which delete only 3′-terminal portions of the *Herc2* transcript, are associated with early juvenile or prenatal lethality, respectively, in homozygous mutant mice. The $p^{17FATWb}$ and $p^{12R250M}$ alleles delete similar amounts of *Herc2*, although the former mutation has also been classified as a prenatal lethal allele (Russell et al. 1995). Both p^{48PB} and p^{9DTW} mice express significant levels of a truncated *Herc2* mRNA, and it is possible that these aberrant transcripts might encode truncated proteins that increase the severity of the *jdf2* phenotype by interfering with factors that bind to and/or interact with *Herc2*. Expression of a defective but otherwise relatively stable protein would not easily explain the severity of the $p^{17FATWb}$ allele, since this mutation deletes all but the 5′-most ~2600 bp of the 15-kb *Herc2* transcript (Table 2, Fig. 2). However, as suggested by these molecular studies, $p^{17FATWb}$ may represent a "skipper" mutation or other type of complex allele, affecting genes that are not immediate neighbors of *Herc2* and *p*. Further studies will be required to determine details of DNA structure and protein expression in this class of mutant alleles.

Finally, these data suggest that sequences required for the proper expression of *p* may be located upstream of the coat color gene, embedded within the body of the *Herc2* transcription unit. One set of potential regulatory sequences is defined by the region deleted in p^{12DTR} DNA. Rearrangements detected in the mottled *p* mutations, p^{39DSD} and p^{103G}, may also point to positions of upstream regulatory sequences required for the proper expression of *p*. The nature of the rearrangements associated with p^{103G} and p^{39DSD} mutations, and the effects these rearrangements may have on *p* expression, are still uncertain. These mutations might, for example, affect *p* gene expression by altering the chromatin structure. Alternatively, by analogy to other mottled mutations, p^{39DSD} might possibly represent an insertion of retroviral sequences (Wu et al. 1997). The insertion of such elements can introduce promoters, enhancers, and other regulatory sequences with long-distance effects on downstream sequences, and sequences disrupted by these rearrangements do not necessarily participate normally in control of *p* gene expression. We can also not exclude that *Herc2* gene product plays some role in *p* expression or function, since even the ENU mutations were induced on a *p*-mutant background (Rinchik et al. 1995). Nevertheless, the present study provides genomic clone reagents and preliminary data required to define the nature and functions of sequences disrupted in these and other p^x, p^m, and *jdf2* alleles.

Acknowledgements. The authors thank Beverly Stanford and Kay Houser for assistance with molecular experiments, and Don Carpenter for advice and help with animal breeding and for sharing personal observations derived from his work with *jdf2* mutant mice. Many thanks to Fiona Francis, Guenther Zehetner, Hans Lehrach, and the RLDB group for access to the mouse P1 library and clones, and to Karin Buiting for many helpful discussions. This work was supported by the U.S. Department of Energy (under contract DE-AC05-96OR22464 with Lockheed-Martin Energy Systems, Inc., to L.B. Russell, D.K. Johnson, E.M. Rinchik, and L. Stubbs, and contract W-7405-Eng-48 with Lawrence Livermore National Laboratory to L. Stubbs), by National Human Genome Research Institute grant no. HG00370 (to E.M. Rinchik), and by a Clinical research grant from the March of Dimes Birth Defects Foundation (to R.D. Nicholls).

References

Buiting K, Greger V, Brownstein BH, Mohr RM, Voiculescu I et al. (1992) A putative gene family in 15q11-13 and 16p11.2: possible implications for Prader-Willi and Angelman syndromes. Proc Natl Acad Sci USA 89, 5457–5461

Culiat CT, Stubbs L, Nicholls RD, Montgomery CS, Russell LB et al. (1993) Concordance between isolated cleft palate in mice and alterations within a region including the gene encoding the beta 3 subunit of the type A gamma-aminobutyric acid receptor. Proc Natl Acad Sci USA 90, 5105–5109

Doyle JL, Ren X, Lennon G, Stubbs L (1997) Mutations in the *Cacnl1a4* calcium channel gene are associated with seizures, cerebellar degeneration, and ataxia in tottering and leaner mutant mice. Mamm Genome 8, 113–120

Gardner JM, Nakatsu Y, Gondo Y, Lee S, Lyon M et al. (1992) The mouse pink-eyed dilution gene: association with human Prader-Willi and Angelman syndromes. Science 257, 1121–1124

Hunt DM, Johnson DR (1971) Abnormal spermiogenesis in two pink-eyed sterile mutants in the mouse. J Embryol Exp Morphol 26, 111–121

Ji Y, Walkowicz MJ, Buiting K, Johnson DK, Tarvin RE et al. (1999) The ancestral Prader-Willi/Angelman syndrome deletion breakpoint region gene encodes a giant protein and is mutated in *jdf2* mice with neuromuscular and spermiogenic abnormalities. Hum Mol Genet 8, 533–542

Johnson DK, Stubbs L, Montgomery CT, Russell LB, Rinchik EM (1995) Molecular analysis of thirty-six mutations at the mouse *p* locus. Genetics 141, 1563–1571

Johnson DR, Hunt DM (1975) Endocrinological findings in sterile pink-eyed mice. J Reprod Fertil 42, 51–58

Lehman AL, Nakatsu Y, Ching A, Bronson RT, Oakey RJ et al. (1998) A very large protein with diverse functional motifs is deficient in *rjs* (runty, jerky, sterile) mice. Proc Natl Acad Sci USA 95, 9436–9441

Lyon MF, King TR, Gondo Y, Gardener JM, Nakatsu Y et al. (1992) Genetic and molecular analysis of recessive alleles at the pink-eyed dilution (*p*) locus of the receptor. Proc Natl Acad Sci USA 89, 6968–6973

Maquat LE (1996) Defects in RNA splicing and the consequence of shortened translational reading frames. Am J Hum Genet 59, 279–286

Marker PC, Seung K, Bland AE, Russell LB, Kingsley DM (1996) Spectrum of *Bmp5* mutations from germline mutagenesis experiments in the mouse. Genetics 145, 435–443

Melvold RW (1974) The effects of mutant *p*-alleles on the reproductive system in mice. Genet Res 23, 319–325

Mueller PR, Wold B (1989) In vivo footprinting of a muscle specific enhancer by ligation mediated PCR. Science 246, 1434–1435

Nicholls RD, Gottlieb W, Russell LB, Davda M, Horsthemke B et al. (1993) Evaluation of potential models for imprinted and nonimprinted components of human chromosome 15q11-q13 syndromes by fine-structure homology mapping in the mouse receptor. Proc Natl Acad Sci USA 90, 2050–2054

Rinchik EM, Carpenter DA, Handel M (1995) Pleiotropy in microdeletion syndromes: neurologic and spermatogenic abnormalities in mice homozygous for the p^{6H} deletion are likely due to dysfunction of a single gene. Proc Natl Acad Sci USA 92, 6394–6398

Russell LB, Montgomery CS, Cacheiro NLA, Johnson DK (1995) Complementation analysis of 45 mutations encompassing the *pink-eyed dilution* locus of the mouse. Genetics 141, 1547–1562

Stubbs L, Huxley C, Hogan B, Evans T, Freid M et al. (1990) The Hox-5 and surfeit gene clusters are linked in the proximal portion of mouse chromosome 2. Genomics 6, 645–650

Wu M, Rinchik EM, Wilkinson JE, Johnson DK (1997) Inherited somatic mosaicism caused by an intracisternal A particle insertion in the mouse tyrosinase gene. Proc Natl Acad Sci USA 94, 890–8941